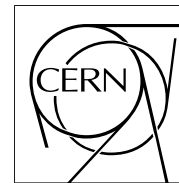


The Compact Muon Solenoid Experiment

# CMS Note

Mailing address: CMS CERN, CH-1211 GENEVA 23, Switzerland



10 May 2006

## 1 Measuring Muon Reconstruction Efficiency from 2 Data

3 D. Acosta<sup>2)</sup>, P. Bartalini<sup>2)</sup>, A. Drozdetskiy<sup>1)2)</sup>, A. Korytov<sup>2)</sup>, G. Mitselmakher<sup>2)</sup>

4 *CMS collaboration*

### 5 Abstract

6 We suggest a method of measuring the global muon reconstruction efficiency  $\epsilon$  directly from data,  
7 which largely alleviates uncertainties associated with our ability to monitor and reproduce in Monte  
8 Carlo simulation all details of the underlying detector performance. With the data corresponding to an  
9 integrated luminosity  $L = 10 \text{ fb}^{-1}$ , and using this method, the precision of measuring  $\epsilon$  for muons in  
10 the  $P_T$  range of 10-100 GeV is expected to be better than 1%.

11 version: 10 May 2006

---

1) Corresponding author, e-mail: [Alexey.Drozdetskiy@cern.ch](mailto:Alexey.Drozdetskiy@cern.ch)

2) University of Florida, Gainesville, FL, USA

# 1 Introduction

Understanding the muon reconstruction efficiency (MRE) with a sub-percent precision at the earlier stages of the CMS operation may be a challenging, if not formidable, task if one attempts to evaluate it by building into the detector simulation all relevant details of detector performance and associated uncertainties. Such simulation would have to include realistic modeling of: geometry, detector edge effects, dead or noisy channels/boards, corrupted data, detectors with turned off or reduced high voltage, luminosity and beam halo, trigger tables. One would need to monitor and incorporate in simulation all, often intermittent, changes in the detector performance.

On the other hand, we can devise a strategy to measure MRE from data in such a way that it would take into account the real detector performance automatically. By choosing a reference process with a large production cross-section (e.g., inclusive Z production), we would be able to reliably measure MRE at the early stage of operation. In this note, we propose such a method and explore its potential in the context of  $H \rightarrow ZZ^{(*)} \rightarrow 4\mu$  analysis [3], where, for obvious reasons, the question of muon efficiency is of very high importance. Reference integrated luminosity used in the note corresponds to the amount of data with which a discovery of the Standard Model Higgs boson may become possible.

Shown below is a feasibility study, which defines a general strategy. The results to be obtained by using this methodology will be applicable to all analyses involving muons of moderate transverse momenta  $P_T$  in the range of 10-100 GeV.

## 2 Strategy for Muon Efficiency Reconstruction from Data

The global muon reconstruction, GMR (the standard CMS algorithm for combining information from the Tracker and Muon sub-systems), is based on *independent* reconstruction of a muon in a standalone Muon system and matching it with a track of similar kinematic parameters in the Tracker. Details on all reconstruction algorithms used in the analysis including GMR can be found in the CMS Physics Technical Design Report, volume 1 [1].

To measure MRE we use a sample of events with at least one muon of  $P_T > 20$  GeV. This value is higher than the High Level Trigger threshold for single muons of 19 GeV [2]. Throughout the paper we call these high  $P_T$  muons ‘‘HLT muons’’. This large data sample consists mostly of  $W \rightarrow \mu\nu$  decays with about 10% of  $Z \rightarrow \mu\mu$  [2]. The production rate is about 10 Hz at  $L = 2 \times 10^{33} \text{ cm}^{-2} \text{ s}^{-1}$ .

Therefore, for the purposes of these studies, we used the inclusive W and Z Monte Carlo (MC) samples from the official CMS production. The inclusive W and Z samples were produced in several  $\hat{P}_T$  bins. For this feasibility study, we selected a sample generated at  $\hat{P}_T$  interval 50 – 85 GeV. Details of the corresponding cross-sections (W/Z were forced to leptonic decay modes) and numbers of expected and simulated events are given in Table 1. Including all other  $\hat{P}_T$  bins would further increase the number of events: full cross section for W/Z-inclusive production is about  $1.5 \cdot 10^5 / 3.9 \cdot 10^4$  pb, which means we should expect of the order of  $10^4$  times larger statistics than number of generated events. Throughout the note we refer to  $10 \text{ fb}^{-1}$  of integrated luminosity for the expected number of events, although the statistical errors are based on the number of simulated events we used shown in Table 1.

Table 1: The W/Z samples used in the study ( $\hat{P}_T$  interval 50 – 85 GeV). Full inclusive cross sections are about  $1.5 \cdot 10^5 / 3.9 \cdot 10^4$  pb.

	inclusive W	inclusive Z
Cross-section $pp \rightarrow W/Z + X$	$1.014 \cdot 10^4$ pb	$1.456 \cdot 10^3$ pb
Number of events for $L = 10 \text{ fb}^{-1}$	$1.014 \cdot 10^8$	$1.456 \cdot 10^7$
Events used in these studies	115,995	93,996
Events in these studies with a muon $P_T > 20$ GeV	18,141	20,247

Starting from this data sample with at least one high- $P_T$  muon (HLT muon), we can reconstruct and histogram invariant masses of the clean trigger muon paired one by one with all tracks found in the Tracker (Fig. 1), all Standalone muons (Fig. 2), and Globally Reconstructed Muons (Fig. 3). The distributions are expected to and do show a distinct peak at  $M_{inv} = M_Z$ ; note the log scale in the Figures. By extrapolating the spectrum from sidebands, we can evaluate the number of  $Z \rightarrow \mu\mu$  events:  $N_{Z(TRK)}$ ,  $N_{Z(SAM)}$ ,  $N_{Z(GMR)}$  in our data sample.

Since the GMR relies on a match between the Stand Alone Muon system and the Tracker, the efficiencies for the three categories are related:

$$\epsilon_{GMR} = \epsilon_{TRK} \cdot \epsilon_{SAM}, \quad (1)$$

where  $\epsilon_{GMR}$  is a Global Muon Reconstruction efficiency,  $\epsilon_{TRK}$  is a track finding efficiency in the Tracker, and  $\epsilon_{SAM}$  is the efficiency of finding a muon in the Stand Alone Muon system. No correlations between Tracker and Muon systems are included as they are two independent systems.

Then, we can write:

$$N_{Z(TRK)} = \epsilon_{HLT} \cdot \epsilon_{TRK} \cdot N_Z, \quad (2)$$

$$N_{Z(SAM)} = \epsilon_{HLT} \cdot \epsilon_{SAM} \cdot N_Z, \quad (3)$$

$$N_{Z(GMR)} = \epsilon_{HLT} \cdot \epsilon_{GMR} \cdot N_Z \quad (4)$$

where  $\epsilon_{HLT}$  is the common, *unknown* efficiency for detecting high  $P_T$  muons and  $N_Z$  is the total *unknown* number of  $Z \rightarrow \mu\mu$  events in our sample. These three equations in combination with Eq.1 can be easily solved for the muon reconstruction efficiency:

$$\epsilon_{GMR} = (N_{Z(GMR)})^2 / (N_{Z(TRK)} N_{Z(SAM)}), \quad (5)$$

$$\epsilon_{TRK} = N_{Z(GMR)} / N_{Z(SAM)}, \quad (6)$$

$$\epsilon_{SAM} = N_{Z(GMR)} / N_{Z(TRK)}. \quad (7)$$

Note that there are two types of efficiencies which enter Eq's 2-4. The first efficiency  $\epsilon_{HLT}$  is for the high- $P_T$  muon preselected by the trigger and our analysis cuts:

- $P_T > 20$  GeV,  $|\eta| < 2.4$
- Muon isolation:  $ISOL_{TRK} < 0.5$  GeV;  $ISOL_{CAL} < 2$  GeV.

Here Tracker-based isolation is defined as  $ISOL_{TRK} = \sum P_T^i$ , where the sum runs over charged particle tracks inside a cone of radius  $R = \sqrt{(\Delta\phi)^2 + (\Delta\eta)^2} = 0.3$  in the azimuth-pseudorapidity space around the muon axis ( $P_T$  of tracks is measured with respect to the beam direction). Calorimeter-based isolation is defined via summing over calorimeter tower  $E_T$ 's in the same cone.

The other efficiencies refer to the offline muon reconstruction. It is those efficiencies that we attempt to measure. We impose the following cuts on the probe muons/tracks (those muons/tracks for which we are calculating efficiencies):  $P_T > 7$  GeV in the barrel region ( $|\eta| < 1.1$ ) or  $P > 13$  GeV in the endcaps ( $1.1 < |\eta| < 2.4$ ). Only such muons are used in the  $H \rightarrow ZZ^{(*)} \rightarrow 4\mu$  analysis to ensure that the muon reconstruction efficiencies are close to their plateau efficiency level (see Figs. 4 and 5), which helps minimize systematic uncertainties.

Also,  $P_T$  and  $P$  ranges of muons in the central and forward directions in the inclusive Z sample (probe muons only) are very similar to those in the  $ZZ \rightarrow 4\mu$  process, the dominant background in the 4-muon Higgs boson decay search (see Figs. 6 and 7), which makes the efficiencies reconstructed in Z-inclusive data samples directly applicable to the ZZ background. Indeed, even average efficiencies for all muons are nearly identical:  $0.972 \pm 0.001$  for Z-inclusive muons and  $0.978 \pm 0.001$  for the ZZ sample (Figs. 6 and 7). Here additional restrictions on two muon invariant mass applied to have similar  $P_T$ -range as in our  $H \rightarrow ZZ^{(*)} \rightarrow 4\mu$  analysis, see Ref. [3].

### 3 Results

Distributions of invariant masses  $M_{inv}(\mu_{HLT} + track)$ ,  $M_{inv}(\mu_{HLT} + \mu_{standalone})$ ,  $M_{inv}(\mu_{HLT} + \mu_{GMR})$  are shown in Figs. 1, 2 and 3. To calculate  $N_{Z(TRK)}$ ,  $N_{Z(SAM)}$ ,  $N_{Z(GMR)}$ , the distributions are fit with an exponential background and a Gaussian signal distribution. In order to reduce the dependence on the shape of the signal  $N_Z$  was estimated from the difference of  $N_{TOT}$ , the total number of entries in the signal region, and  $N_B$  as derived from the background part of the fit. The signal region was extending to  $\pm 6\sigma$  GeV around the fitted mean value of the Gaussian distribution. Expectations for  $N_{TOT}$ ,  $N_B$  and  $N_Z = N_{TOT} - N_B$  are summarized in

Table 2: Number of expected events at  $L = 10 \text{ fb}^{-1}$  in the  $M_Z$  peak signal region,  $N_{TOT}$ ; background (accidental) pairings,  $N_B$ ; and reconstructed  $Z \rightarrow 2\mu$  events,  $N_Z$ . The error on  $N_B$  is for the actual statistics used in these studies ( $L \sim 0.01 \text{ fb}^{-1}$ ). See text for details.

	HLT+GMR	HLT+SAM	HLT+TRK
$N_{TOT}$	2,070,000	2,270,000	4,360,000
$N_B$	150,000	340,000	2,410,000
$N_Z = N_{TOT} - N_B$	1,920,000	1,930,000	1,950,000
$\delta N_B$	$\sim 30,000$	$\sim 30,000$	$\sim 100,000$

76 Table 2. In future studies systematic uncertainties in the determination of the background should be determined,  
77 either by varying the functions used in the fit or by comparing  $N_B$  with the number obtained from simulation.

78 The errors on  $N_B$ ,  $\delta N_B$ , are defined by the actual statistics used in these studies, approximately corresponding  
79 to  $L = 0.01 \text{ fb}^{-1}$ . It is these errors that drive the total statistical uncertainty on the measured efficiencies. We  
80 calculate the statistical uncertainty on the efficiencies assuming independent measurements of the event counts:

$$\frac{\delta\epsilon_{GMR}}{\epsilon_{GMR}} = 2 \frac{\delta N_B(GMR)}{N_Z(GMR)} \oplus \frac{\delta N_B(TRK)}{N_Z(TRK)} \oplus \frac{\delta N_B(SAM)}{N_Z(SAM)}, \quad (8)$$

$$\frac{\delta\epsilon_{TRK}}{\epsilon_{TRK}} = \frac{\delta N_B(GMR)}{N_Z(GMR)} \oplus \frac{\delta N_B(SAM)}{N_Z(SAM)}, \quad (9)$$

$$\frac{\delta\epsilon_{SAM}}{\epsilon_{SAM}} = \frac{\delta N_B(GMR)}{N_Z(GMR)} \oplus \frac{\delta N_B(TRK)}{N_Z(TRK)} \quad (10)$$

81 Given the sample we use in these studies, the measured Global Muon Reconstruction efficiency is  $\epsilon_{GMR} = 0.983 \pm$   
82  $0.062$ . Table 3 shows that the measured efficiency agrees very well with the efficiency that we can reconstruct from  
83 comparing the reconstructed muons with generator MC truth muons. This is the main result of these studies. With  
84 more than  $10^3 - 10^4$  times larger statistics (increase in statistics expected for  $L = 10 \text{ fb}^{-1}$  with respect to the  
85 number of generated events we use in this study), one can sub-divide the full statistics in a grid of  $\eta$ ,  $\phi$  and  $P_T$   
86 regions and still be able to measure efficiency in each of them with a sub-percent precision. Such sub-division will  
87 also automatically show all “cracks” in  $\eta - \phi - P_T$  space in the detector sensitivity, where the detector sensitive  
88 parts in  $\eta - \phi - P_T$  space can be defined as sensitive areas for GMR HLT isolated (high quality) muons. Note that  
89 the  $P_T/P$  and  $\phi$  dependencies of muon efficiency are almost flat and would not need fine binning. Note also that  
90 the method automatically includes possible sources of systematic uncertainties like fakes, misidentified muons and  
91 all other sorts of “background contamination” as those tracks do not have a distinct feature of peaking around  $Z^0$   
92 invariant mass and hence will be subtracted by the procedure as we perform calibration to side bands.

Table 3: Measured muon efficiencies ( $L = 0.01 \text{ fb}^{-1}$ ) and those obtained from comparing reconstructed muons with MC truth muons.

	GMR	SAM	TRK
$\epsilon$ from $Z$ inclusive data	$0.983 \pm 0.062$	$0.986 \pm 0.054$	$0.997 \pm 0.022$
$\epsilon$ in $Z$ inclusive MC sample	$0.972 \pm 0.001$	N/A	N/A
$\epsilon$ in $ZZ$ MC sample	$0.978 \pm 0.001$	N/A	N/A

## 93 4 Summary

94 A method of measuring the global muon reconstruction efficiency  $\epsilon$  directly from data was studied. With the  
95 data corresponding to an integrated luminosity  $L = 10 \text{ fb}^{-1}$ , the precision of measuring  $\epsilon$  for muons in the  $P_T$   
96 range of  $10 - 100 \text{ GeV}$  is expected to be better than 1%, potentially much better. The method largely alleviates  
97 uncertainties associated with our ability to monitor and reproduce in Monte Carlo simulation all details of the  
98 underlying detector performance.

99 The CMS simulation/reconstruction software is undergoing a major changeover in preparations for data taking.  
100 As the new Monte Carlo samples produced in the new software framework become available, the studies will be

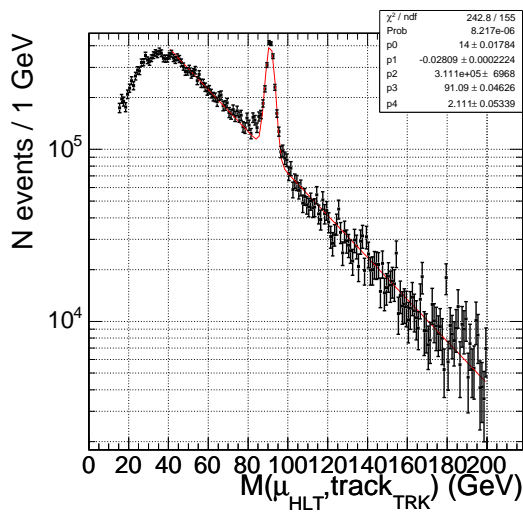


Figure 1: Invariant mass distribution:  $M(\mu_{HLT}, track_{TRK})$  for HLT muon and Tracker track.

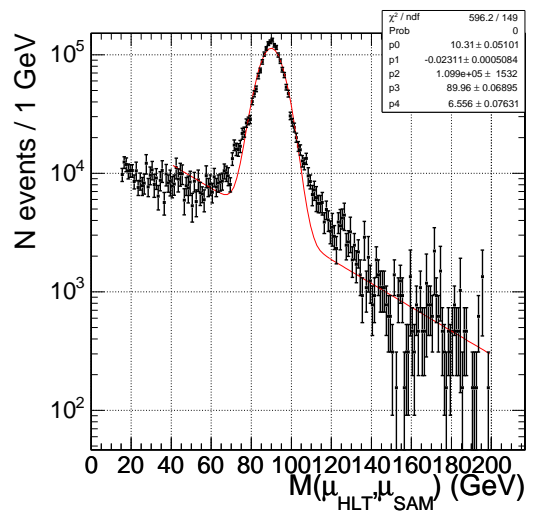


Figure 2: Invariant mass distribution:  $M(\mu_{HLT}, \mu_{SAM})$  for HLT muon and Standalone Muon Reconstructor muon.

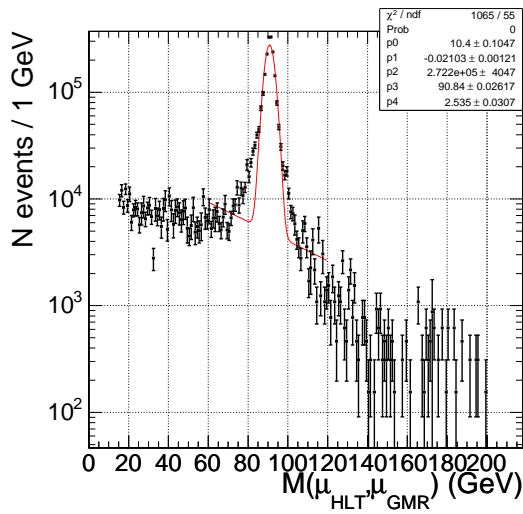


Figure 3: Invariant mass distribution:  $M(\mu_{HLT}, \mu_{GMR})$  for HLT muon and another Global Muon Reconstructor muon.

101 updated with much larger statistics that will also allow us to evaluate possible systematic errors at sub-percent  
 102 level.

## 103 5 Acknowledgments

104 We would like to thank W. Adam, T. Cox, J. Mumford, N. Neumeister and T. Todorov for useful discussions.

## 105 References

- 106 [1] CMS Collaboration, “The CMS Physics Technical Design Report, Volume 1”, CERN/LHCC, 2006.  
 107 [2] CMS Collaboration, “The Trigger and Data Acquisition project”, v.2, p.308, 2002 (see Fig. 15-21)  
 108 [3] S. Abdullin et al., “Search for  $H \rightarrow ZZ^{(*)} \rightarrow 4\mu$  Using  $M(4\mu)$ -Dependent Cuts”, CMS Note in preparation,  
 109 2006.

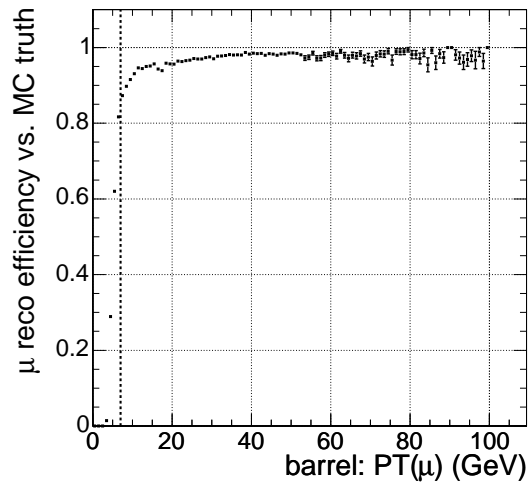


Figure 4: Global Muon Reconstruction efficiency calculated from matching reconstructed and Monte Carlo truth muons in the barrel region for ZZ events.

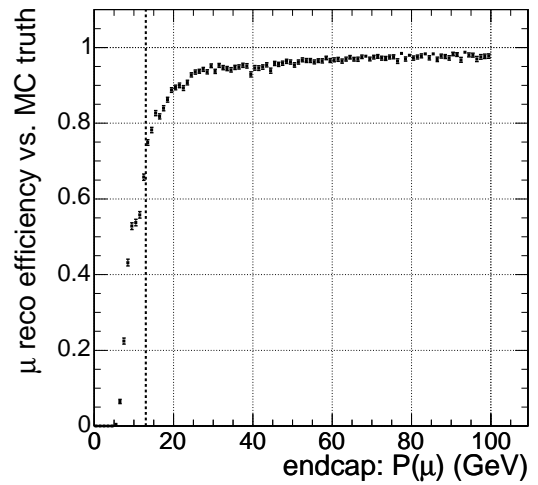


Figure 5: Global Muon Reconstruction efficiency calculated from matching reconstructed and Monte Carlo truth muons in the endcap region for ZZ events.

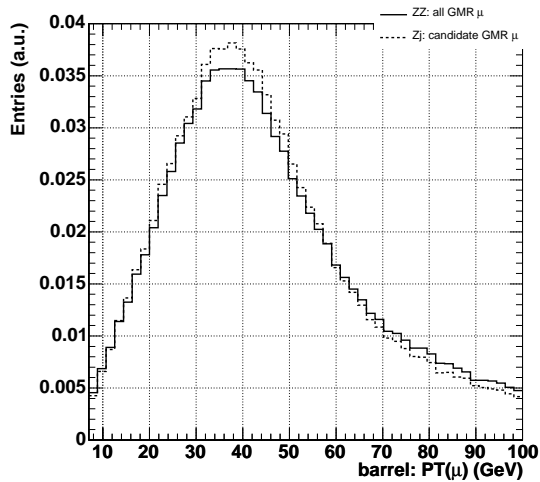


Figure 6: Muon  $P_T$  spectrum in the barrel region for ZZ (solid line) and Z (dashed lines) events.

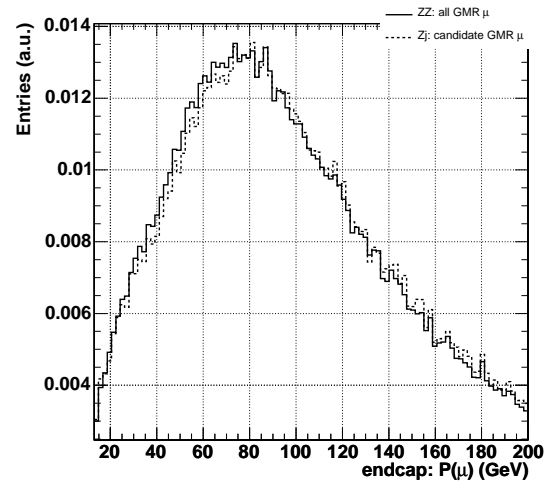


Figure 7: Muon  $P$  spectrum in the endcap region for ZZ (solid line) and Z (dashed lines) events.